Biuletyn WAT
Vol. LXVII, Nr 2, 2018

Dynamic displacement analysis of reinforced concrete deep beams made of high strength concrete

Part II: Dynamic displacement analysis of reinforced concrete deep beams made of high strength *C200* grade concrete

WALDEMAR CICHORSKI

Military University of Technology, Faculty of Civil Engineering and Geodesy,
2 Gen. W. Urbanowicza Str., 00-908 Warsaw, waldemar.cichorski@wat.edu.pl

Abstract. The dynamic load displacements were analysed of rectangular concrete deep beams made of very high strength concrete, grade *C200,* including an evaluation of the physical non-linearity of the construction materials: concrete and reinforcing steel. The analysis was conducted using the method presented in [1]. The numerical calculation results are presented with particular reference to the displacement state of rectangular concrete deep beams. A comparative analysis was conducted on the effect of the high-strength concrete and the steel of increased strength on a class *C200* concrete deep beam versus the results produced in [10] for a class *C100* concrete deep beam.
Key words: mechanics of structures, reinforced concrete structures, deep beams, dynamic load, physical non-linearity
DOI: 10.5604/01.3001.0012.0952

1. Introduction

The purpose of this work was to analyse the effects of very high-strength concrete and increased-strength reinforcing steel on the displacement of rectangular reinforced-concrete deep beams under dynamic loads, with consideration of the physical non-linearity of the concrete and reinforcing steel used as the construction materials. The assumptions adopted for structural modelling of the construction materials and the method chosen for the solution are explained in Part One of this work, [10]. The subject of this analysis, the geometric features of the deep beams, the material parameters of the concrete and of the reinforcing steel, and the estimation of the static

carrying capacity levels of specific deep beam types, as determined per [9], are also shown in Part One, [10]. This paper focuses on an analysis of the deformation of rectangular deep beams made from class *C200* concrete, reinforced with standard reinforcement steel in one version and with increased-strength reinforcement steel in another version. The comparative analysis of the results included the results from the analysis of effort of the reinforced concrete deep beam made with *C100* concrete, presented in [10].

2. Analysis of numerical results

To illustrate the effect of very high-strength concrete on the displacement state of rectangular reinforced concrete deep beams, numerical experiments were carried out on the deep beam with the reinforcement arranged as in the experiment [6] and with modified parameters describing the constitutive concrete model (in this part, concrete class *C200* was used). Additionally, the effect of changing the strength parameters of the reinforcing steel, i.e. the influence of replacing class *A-III* standard steel, as used in [6], with increased-strength steel (class *A-H*), was analysed.

For this purpose, the following points in the central section (designated in Fig. 1) were adopted for the observation of dynamic changes in the displacement of the deep

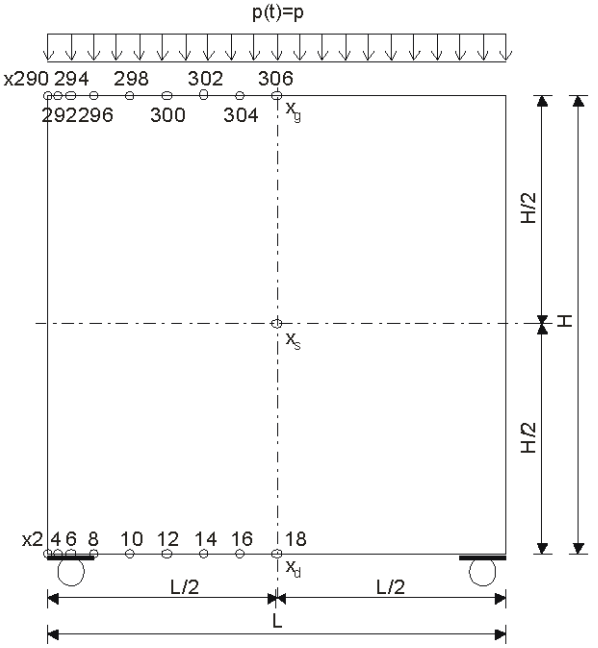

Fig. 1. Locations of the points for displacement observation

beam: x_d — on the lower edge, x_s — in the centre of the deep beam height, and x_g — on the upper edge. In turn, the following points were selected for observation in order to illustrate the variability over time of the lower and upper edge of the deep beam:

— on the lower edge of the deep beam: x_2, x_4, x_6, x_8, x_{10}, x_{12}, x_{14}, x_{16}, x_{18};
— on the upper edge of the deep beam: x_{290}, x_{292}, x_{294}, x_{296}, x_{298}, x_{300}, x_{302}, x_{304}, x_{306};

the locations of which are show in Fig. 1.

2.1. Reinforced-concrete deep beam reinforced with standard class steel (A-III)

Fig. 2 shows the variability of vertical displacement over time of selected points in the central section at various load levels, $\alpha = P/P_0$. Up to the load level $\alpha = 0.3$, Fig. 2_1 and Fig. 2_2, not unlike in a reinforced concrete deep beam made from *C100* concrete, the structure reacted in the elastic range at the low level of inelastic processes in the concrete; the results indicated an analogical relation between the vertical displacements: $v(x_g) > v(x_s) > v(x_d)$. As the load increased to the level $\alpha = 0.4$, Fig. 2_3, an increase in the vertical displacements at the lower point x_d was observed. Because of the cracks (scratching) of the concrete in the lower layers of the shear zone, a partial modification was used for the interrelation of the changes of individual vertical displacements over time: $v(x_g) > v(x_d) \cong v(x_s)$. As the load was increased to $\alpha = 0.5$, Fig. 2_4, propagation of the crack areas occurred in a different manner than the propagation in the *C100* concrete deep beam, in that the propagation was observed in the shear zone only (and in two directions: upward and diagonally toward the span centre). The effect of this was unlike that of the *C100* concrete deep beam: it did not modify the interrelation of the changes of individual vertical displacements over time, i.e. $v(x_g) > v(x_d) \cong v(x_s)$. At the load level of $\alpha = 0.6$, Fig. 2_5 (not unlike in the *C100* concrete deep beam), the lack of stabilisation of the plastic processes was observed and manifested as a lack of a stabilized vibrating movement around the permanent displacements of the observed points. As an effect of the development of the concrete crack zones in one area, diagonally from the shear zone to the upper layers of the span cross-section, the carrying capacity of the deep beam was lost.

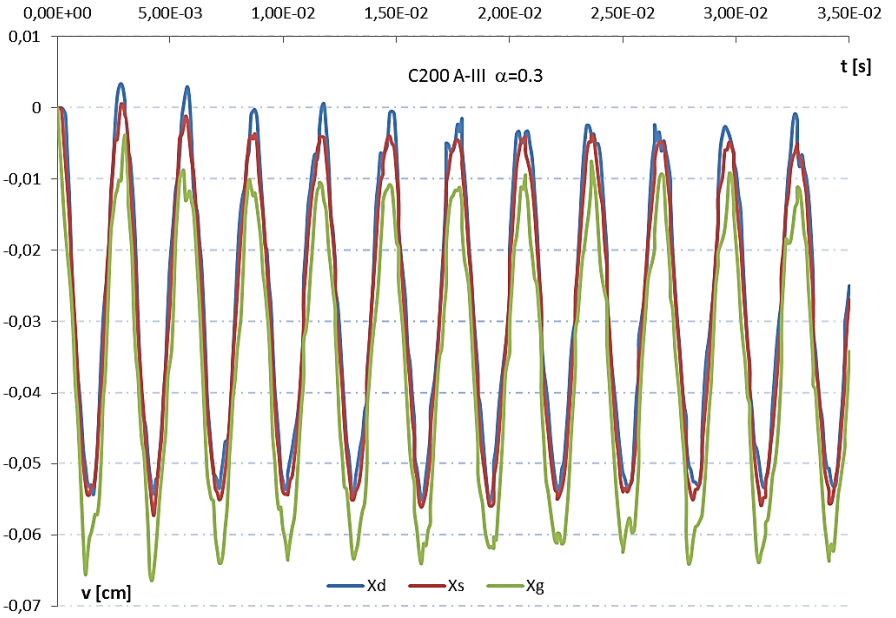

Fig. 2_1. Change in vertical displacements over time of the points in the central section at the load level $\alpha = 0.1$

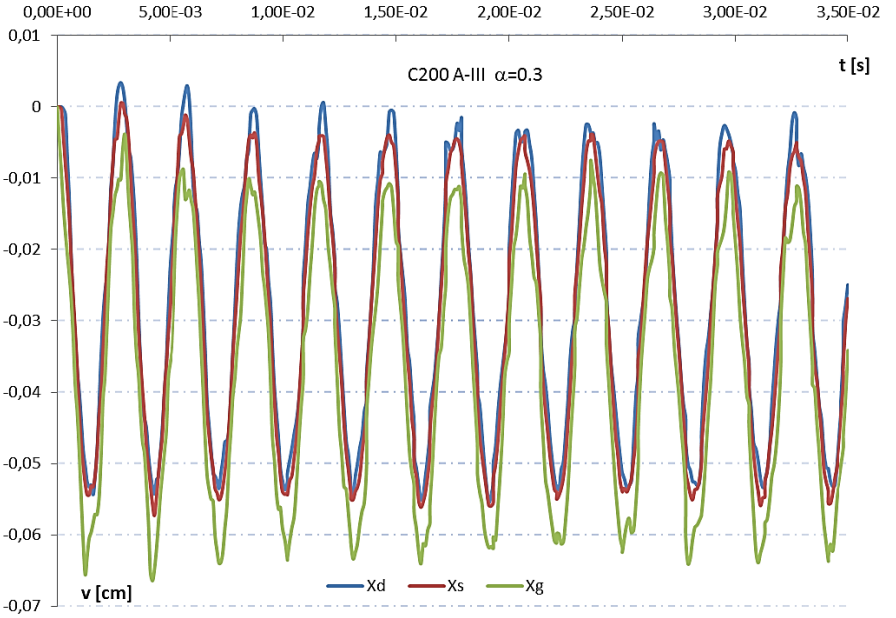

Fig. 2_2. Change in vertical displacements over time of the points in the central section at the load level $\alpha = 0.3$

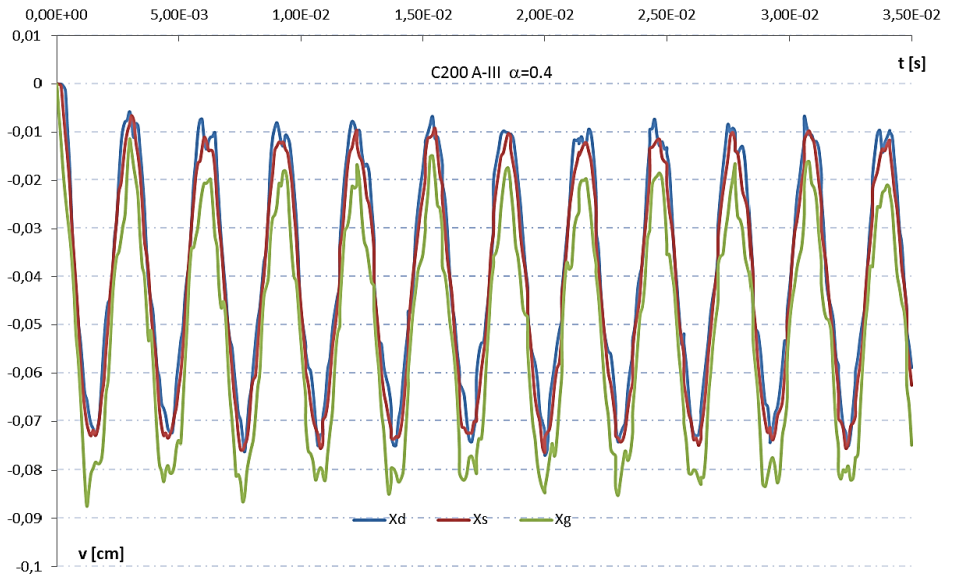

Fig. 2$_3$. Change in vertical displacements over time of the points in the central section at the load level $\alpha = 0.4$

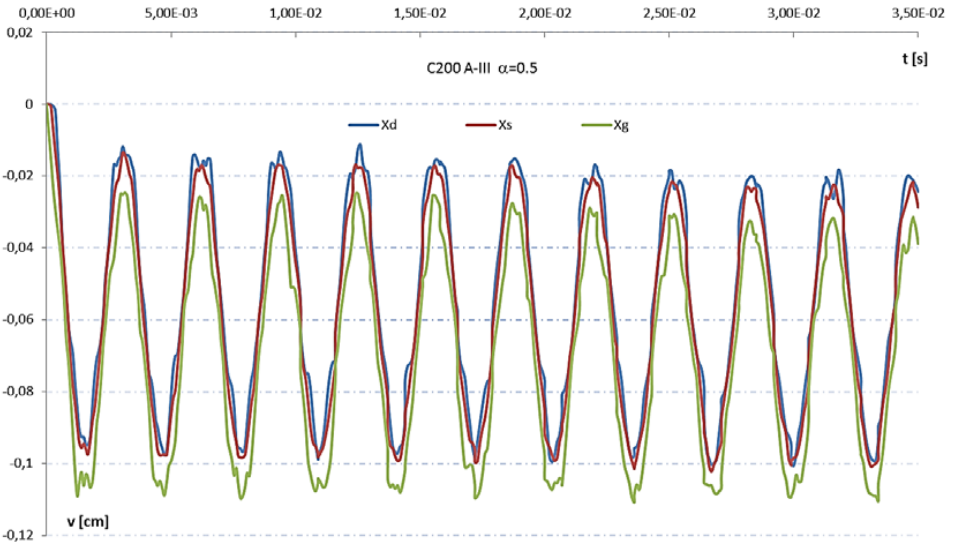

Fig. 2$_4$. Change in vertical displacements over time of the points in the central section at the load level $\alpha = 0.5$

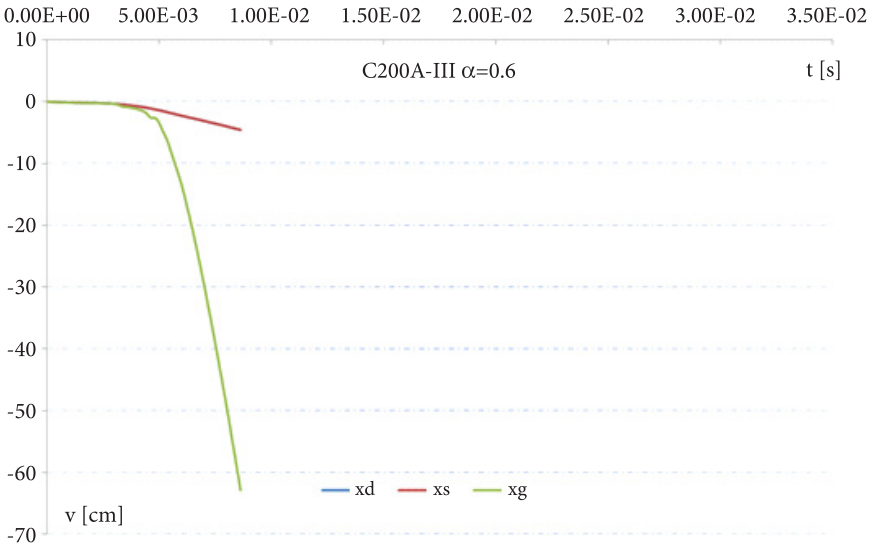

Fig. 2_5. Change in vertical displacements over time of the points in the central section at the load level $\alpha = 0.6$

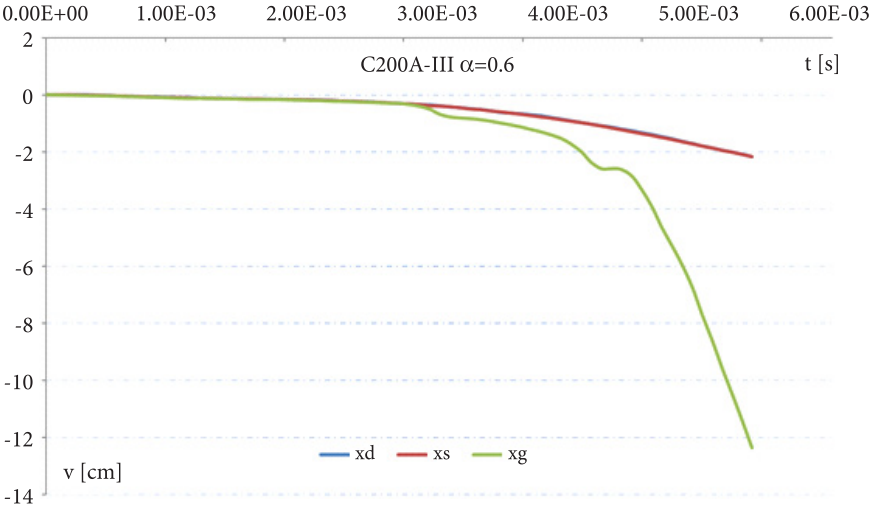

Fig. 2_{5a}. Change in the vertical displacements over time of the points in the central section at the load level $\alpha = 0.6$ — a limited time interval was applied to the results in Fig. 2_5

Fig. 3 shows the variability of the vertical displacement over time of the selected points at the lower edge of the deep beam at different load levels, $\alpha = P/P_0$. In the range of the elastic capacity of the structure, load $a = 0.1$ and $a = 0.2$ gave the maximum deflection, the same as for the *C100* concrete deep beam span at point x_{18}, and the observed amplitude values of the vertical displacements decreased monotonously towards the support. The same behaviour of the structure was observed at load level $a = 0.3$, (Fig. 3_1), when the cracking of the concrete in the proximity of the support occurred. At load level $a = 0.4$, (Fig. 3_2), and unlike for the *C100* concrete deep beam, the previous relation was observed: the maximum deflection was at point x_{18} of the span at lower load levels, and the observed amplitudes of vertical displacements decreased monotonously towards the support. At load level $a = 0.5$, (Fig. 3_3), and unlike for the *C100* concrete deep beam, the previous relation was observed: no indications of concrete cracks were found in the central section at lower load levels, unlike for the *C100* concrete deep beam. In Fig. 3_4, with load level $a = 0.6$, further development of the concrete cracking area was found. There was an unlimited increase in the vertical displacements at the points adjacent to the span cross-section, indicative of the carrying capacity limit with a failure of the deep beam.

Fig. 4 shows the variability of the vertical displacement over time at the selected points at the upper edge of the deep beam at different load levels, $\alpha = P/P_0$. At load levels $a = 0.1$, $a = 0.2$, (Fig. 4_1), $a = 0.3$, (Fig. 4_2) and $a = 0.4$, the maximum deflection was at point x_{306} of the span, and the observed amplitude values of the vertical displacements decreased monotonously towards the support. The same behaviour of the structure was observed at load level $a = 0.5$, (Fig. 4_3); however, unlike in the *C100* concrete deep beam, there was no evidence of dynamic balance differentiation, i.e. no permanent displacement of the points on the upper edge occurred. In Fig. 4_4, with load level $a = 0.6$, further development of the concrete cracking area was found. There was an unlimited increase in the vertical displacements at the points in the vicinity of point x_{300}, indicative of the carrying capacity limit with a failure of the deep beam.

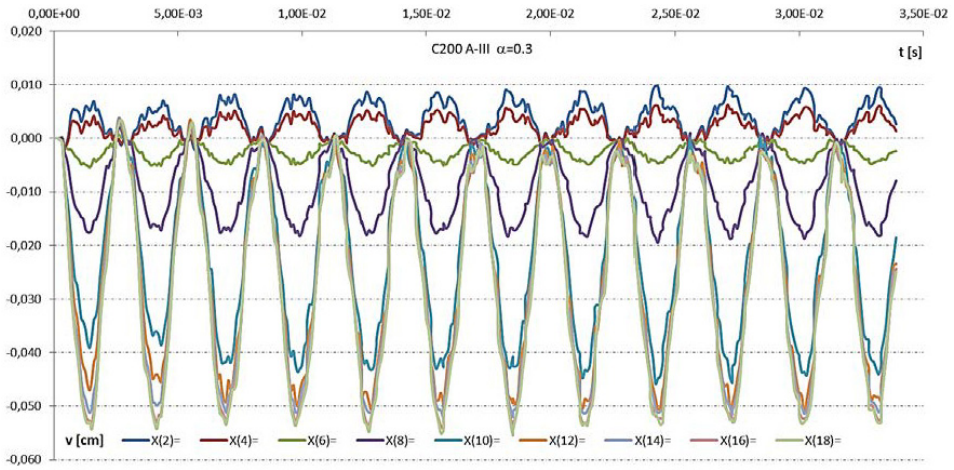

Fig. 3_1. Change in vertical displacements over time of the points at the lower edge of the deep beam at the load level $\alpha = 0.3$

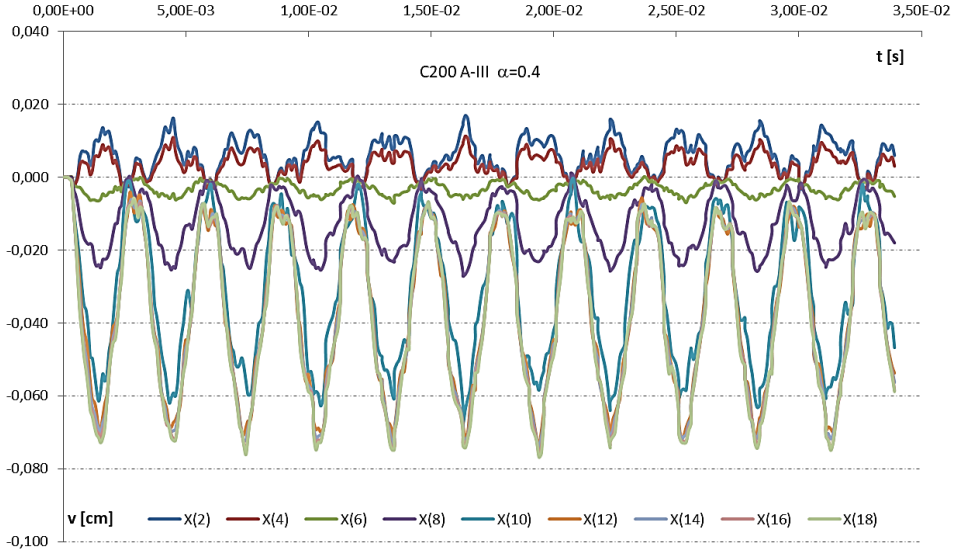

Fig. 3_2. Change in vertical displacements over time of the points at the lower edge of the deep beam at the load level $\alpha = 0.4$

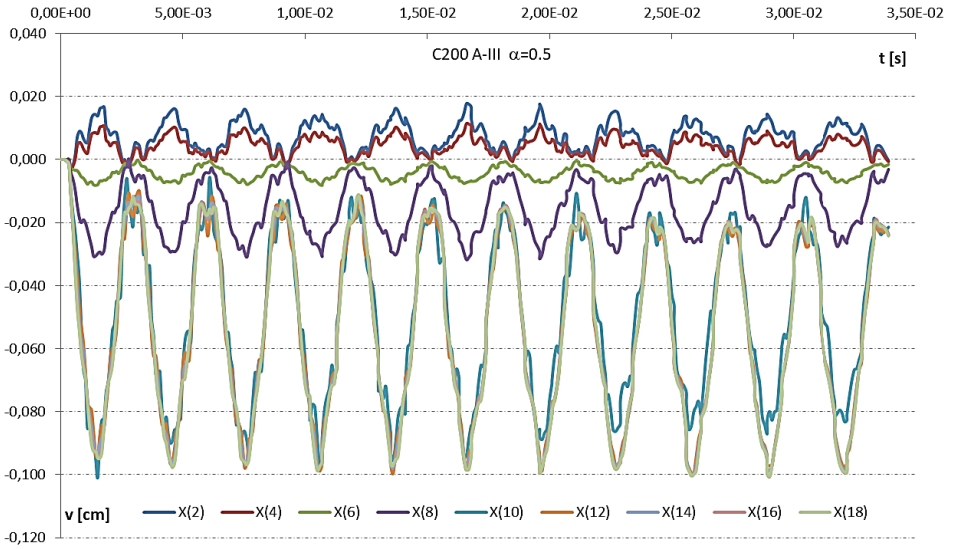

Fig. 3_3. Change in vertical displacements over time of the points at the lower edge of the deep beam at the load level $\alpha = 0.5$

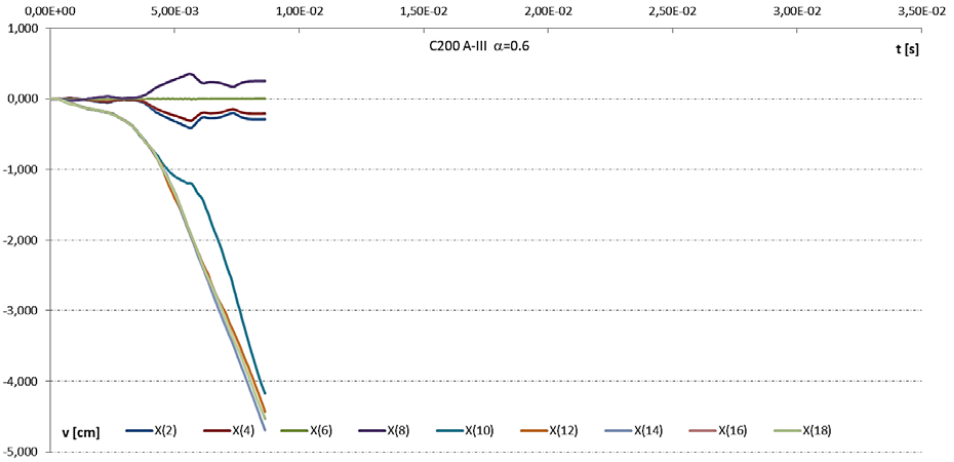

Fig. 3_4. Change in vertical displacements over time of the points at the lower edge of the deep beam at the load level $\alpha = 0.6$

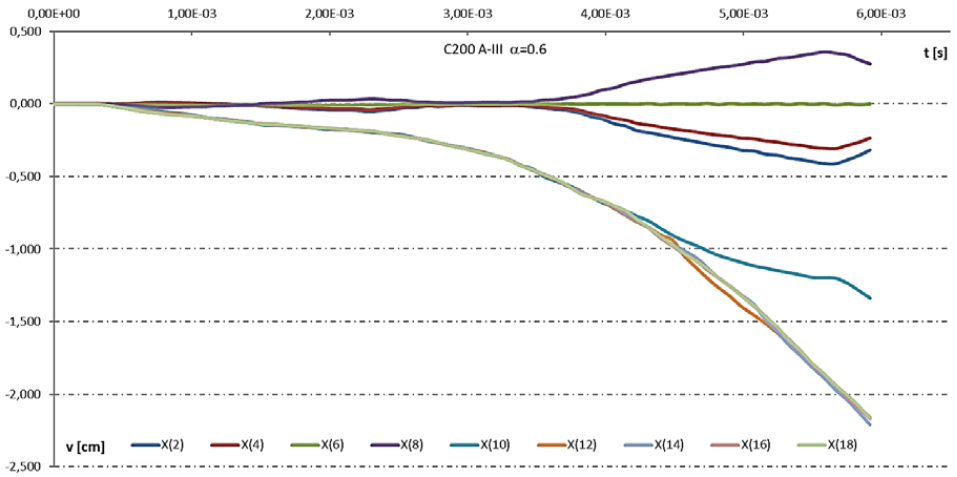

Fig. 3_{4a}. Change in vertical displacements over time of the points at the lower edge of the deep beam at the load level $\alpha = 0.6$ — a limited time interval was applied to the results in Fig. 3_4

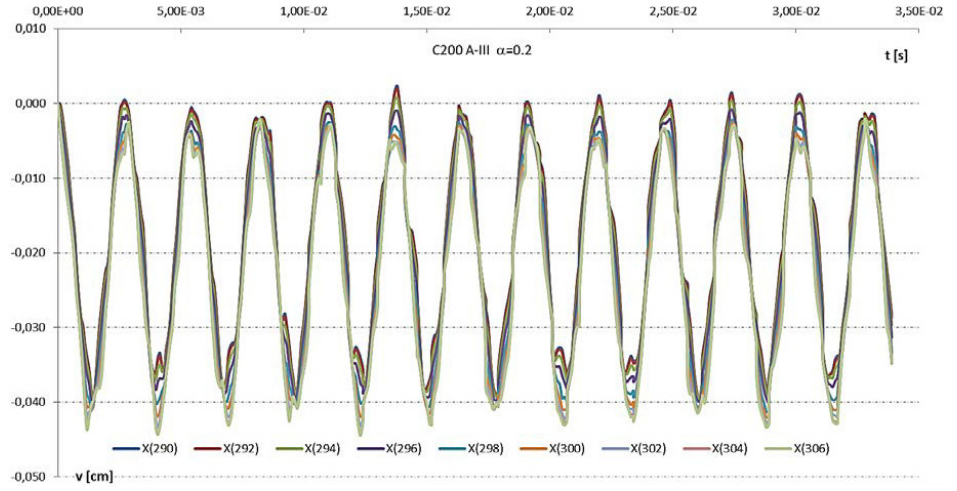

Fig. 4_1. Change in vertical displacements over time of the points at the upper edge of the deep beam at the load level $\alpha = 0.2$

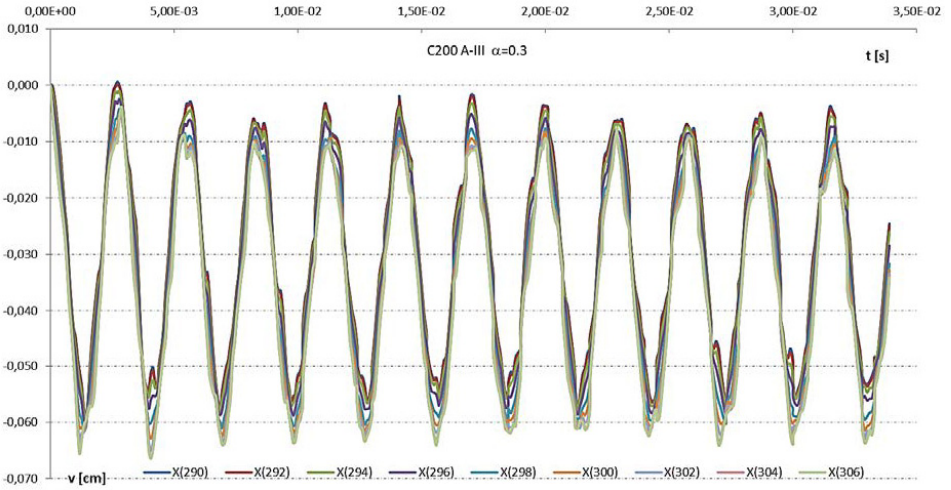

Fig. 4_2. Change in vertical displacements over time of the points at the upper edge of the deep beam at the load level $\alpha = 0.3$

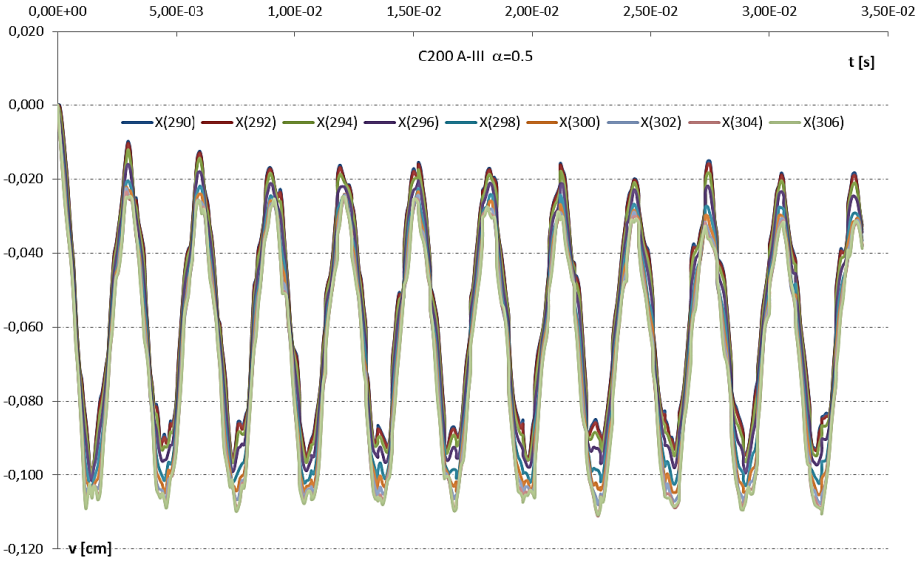

Fig. 4_3. Change in vertical displacements over time of the points at the upper edge of the deep beam at the load level $\alpha = 0.5$

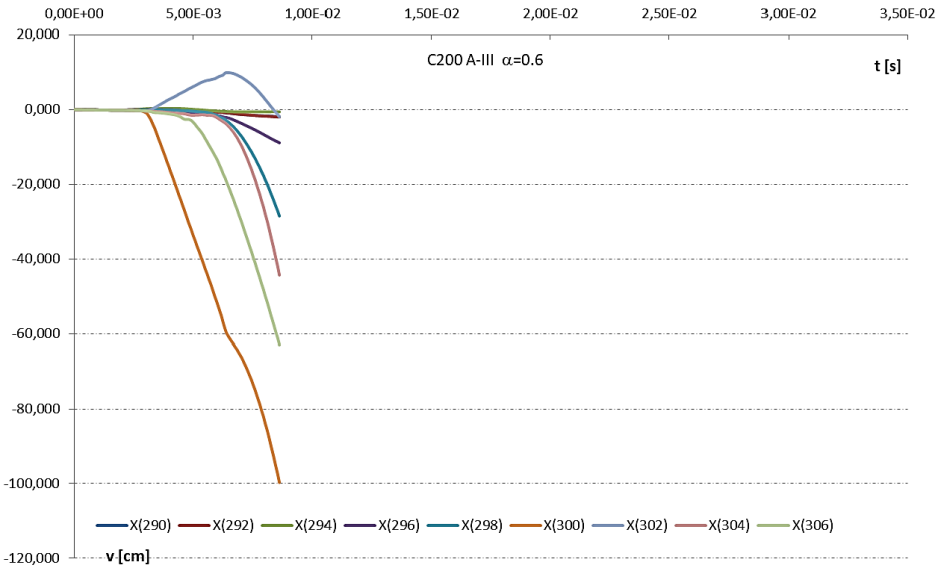

Fig. 4_4. Change in vertical displacements over time of the points at the upper edge of the deep beam at the load level $\alpha = 0.6$

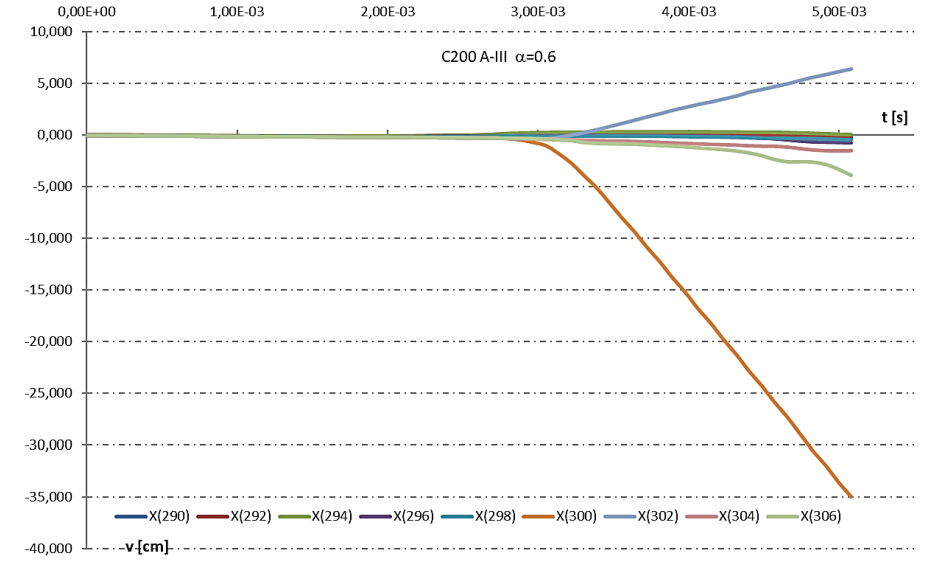

Fig. 4_{4a}. Change in vertical displacements over time of the points at the upper edge of the deep beam at the load level $\alpha = 0.6$ — a limited time interval was applied to the results in Fig. 4_4

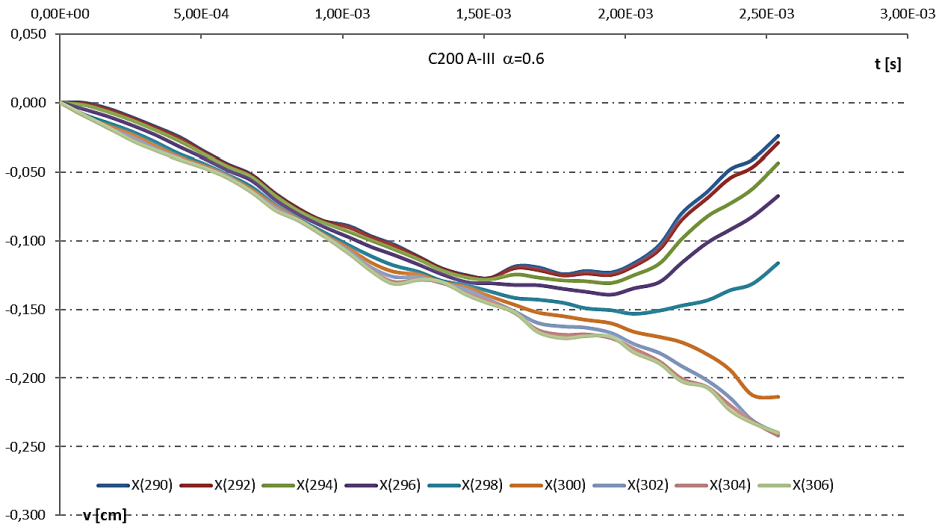

Fig. 4_{4b}. Change in vertical displacements over time of the points at the upper edge of the deep beam at the load level α= 0.6 — a limited time interval was applied to the results in Fig. 4_{4a}

2.2. Reinforced-concrete deep beam reinforced with standard class steel (A-H)

Fig. 5 shows the variability of the vertical displacement over time at selected points in the central section at various load levels, $\alpha = P/P_0$. Up to load level $\alpha = 0.3$, Fig. 5_1 and Fig. 5_2, similar to the reinforced concrete deep beam with *A-III* reinforcing steel, the structure reacted in the elastic range at a low level of plastic processes in the concrete; the results indicated an analogical relation between the vertical displacements: $v(x_g) > v(x_s) > v(x_d)$. As the load increased to level $\alpha = 0.4$, Fig. 5_3, an increase in the vertical displacements at the lower point x_d was observed. Because of the cracks (scratching) of the concrete in the lower layers of the shear zone, a partial modification was made for the interrelation of changes in the individual vertical displacements over time, not unlike in the *A-III* steel reinforced deep beam: $v(x_g) > v(x_d) \cong v(x_s)$. As the load was increased to $\alpha = 0.5$, fig. 5_4, propagation of the crack areas occurred analogically to that in the reinforced concrete deep beam, reinforced with *A-III* steel, in the shear zone only (and in two directions: upward and diagonally toward the span centre). This effect was similar to the *A-III* steel reinforced deep beam: it did not modify the interrelation of the changes in the individual vertical displacements over time, i.e. $v(x_g) > v(x_d) \cong v(x_s)$. As an effect of the development of the concrete cracking zones within a single area only, similar to the deep beam reinforced with *A-III* steel, i.e. diagonally from the shear zone to the upper layers of the span cross-section, the carrying capacity was lost at this load level, unlike the effect in the *A-III* steel reinforced deep beam. The maximum load level was changed by the replacement of reinforcing steel grade *A-III* with grade *A-H*.

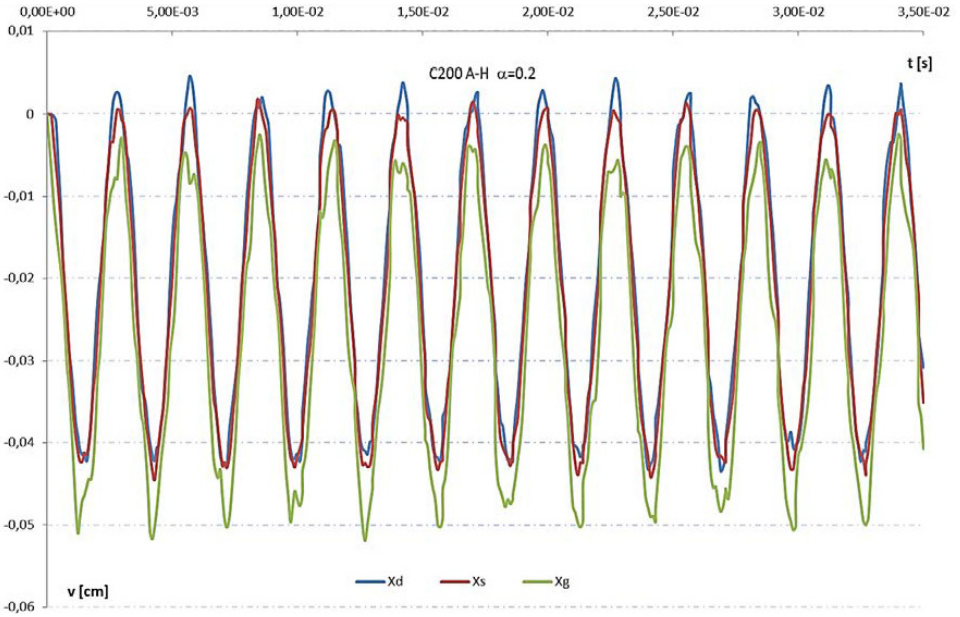

Fig. 5_1. Change in vertical displacements over time of the points in the central section at the load level $\alpha = 0.2$

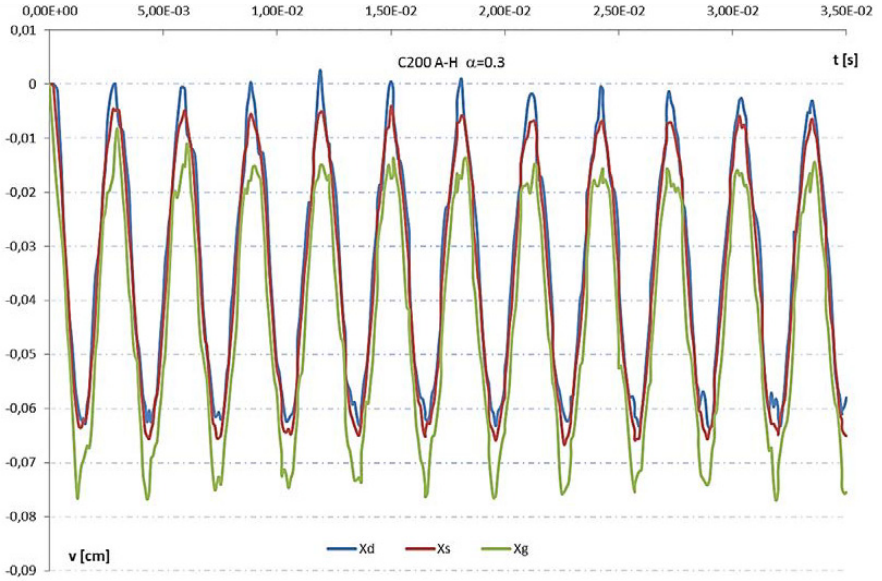

Fig. 5_2. Change in vertical displacements over time of the points in the central section at the load level $\alpha = 0.3$

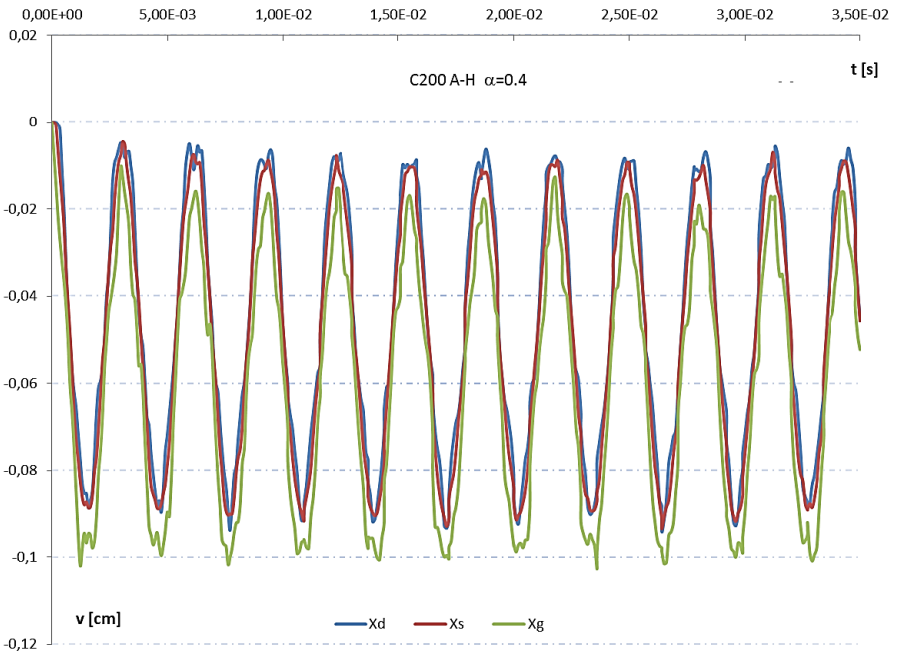

Fig. 5_3. Change in vertical displacements over time of the points in the central section at the load level $\alpha = 0.4$

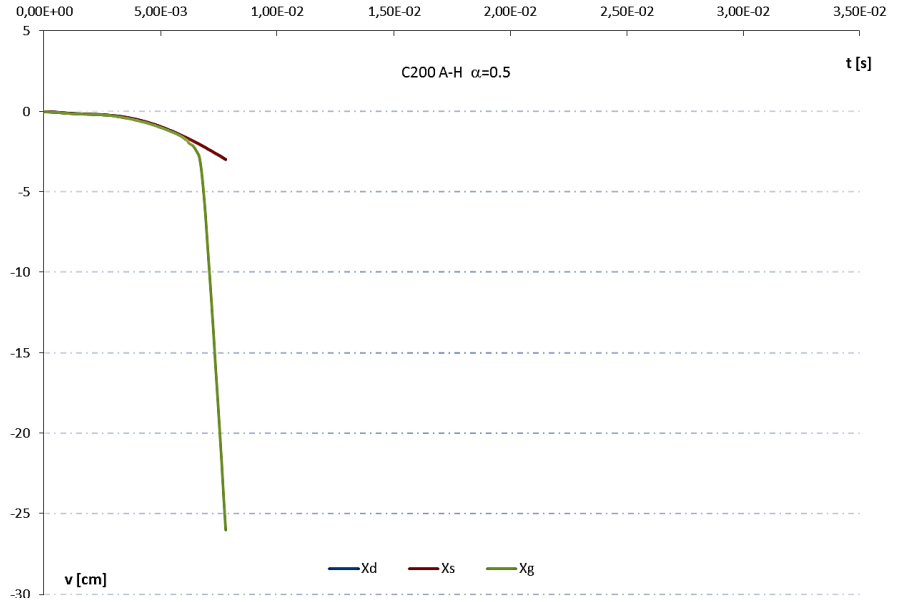

Fig. 5_4. Change in vertical displacements over time of the points in the central section at the load level $\alpha = 0.5$

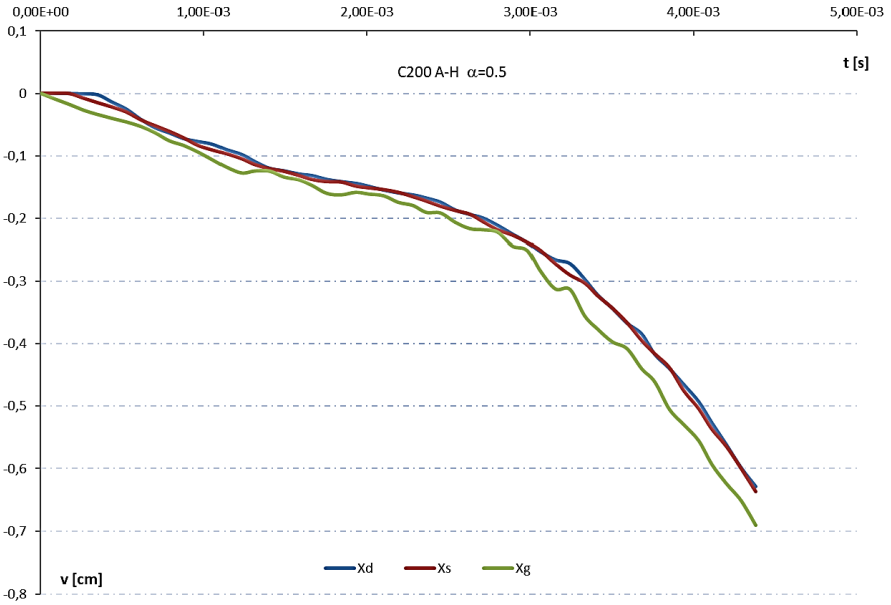

Fig. 5_{4a}. Change in the vertical displacements over time of the points in the central section at the load level $\alpha = 0.5$ — a limited time interval was applied to the results in Fig. 5_4

Fig. 6 shows the variability of the vertical displacement over time of the selected points at the lower edge of the deep beam at different load levels, $\alpha = P/P_0$. In the range of elastic capacity of the structure, load $a = 0.1$ and $a = 0.2$, gave the maximum deflection, the same as with the *A-III* steel reinforced deep beam span at point x_{18}, and the observed amplitude values of the vertical displacements decreased monotonously towards the support. The same behaviour of the structure was observed at load level $a = 0.3$, (Fig. 6_1), when the cracking of the concrete in the proximity of the support occurred. At load level $a = 0.4$, (Fig. 6_2) and similar to the *A-III* steel reinforced deep beam, the previous relation was observed: the maximum deflection was at point x_{18} of the span at lower load levels, and the observed amplitudes of vertical displacements decreased monotonously towards the support. In Fig. 6_3, which shows load level $a = 0.5$, further development of the concrete cracking area was found. Unlike in the deep beam reinforced with *A-III* steel, there was an unlimited increase in the vertical displacements at the points adjacent to the span cross-section and indicative of the carrying capacity limit with a failure of the deep beam.

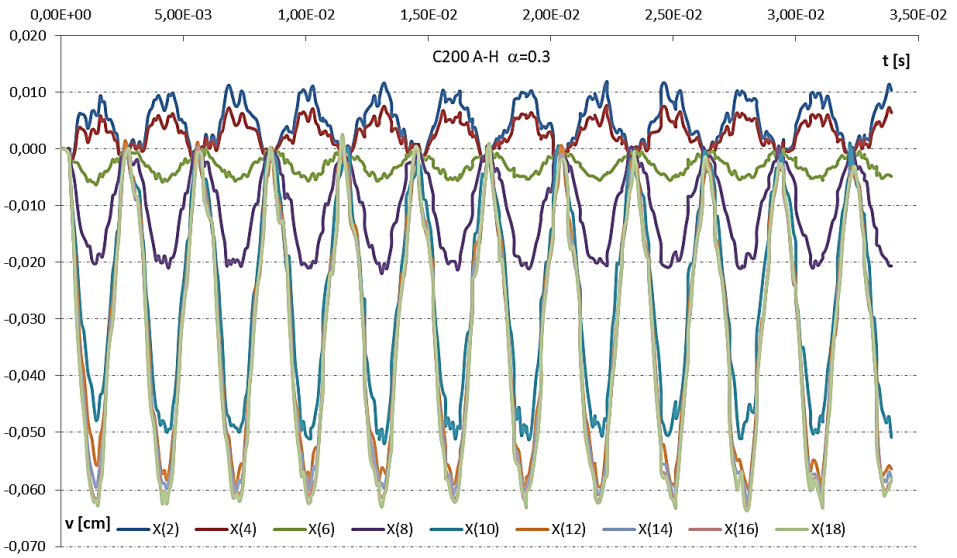

Fig. 6_1. Change in vertical displacements over time of the points at the lower edge of the deep beam at the load level $\alpha = 0.3$

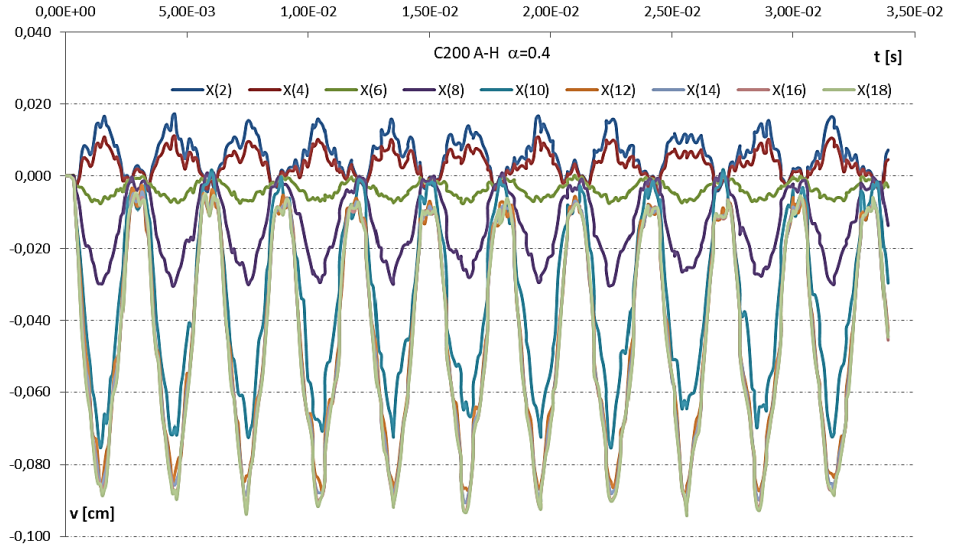

Fig. 6_2. Change in vertical displacements over time of the points at the lower edge of the deep beam at the load level $\alpha = 0.4$

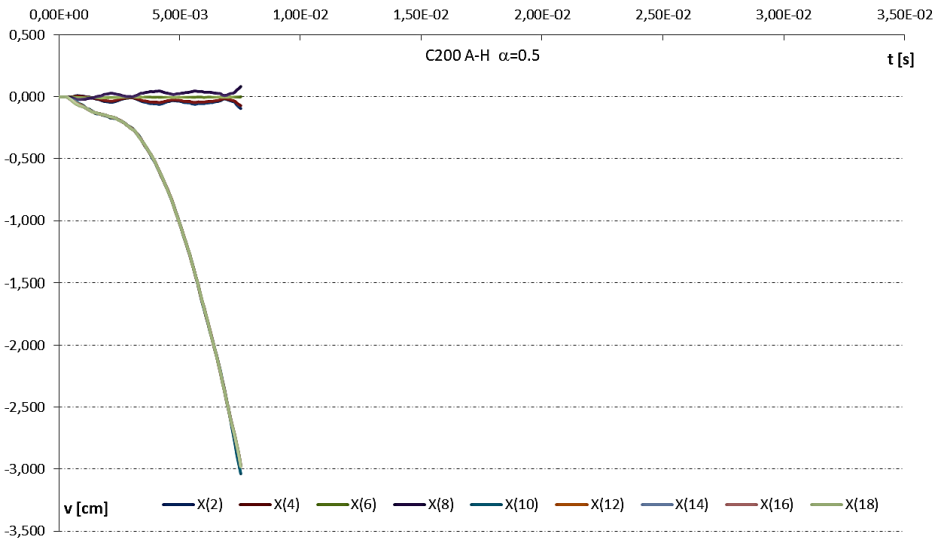

Fig. 6_3. Change in vertical displacements over time of the points at the lower edge of the deep beam at the load level $\alpha = 0.5$

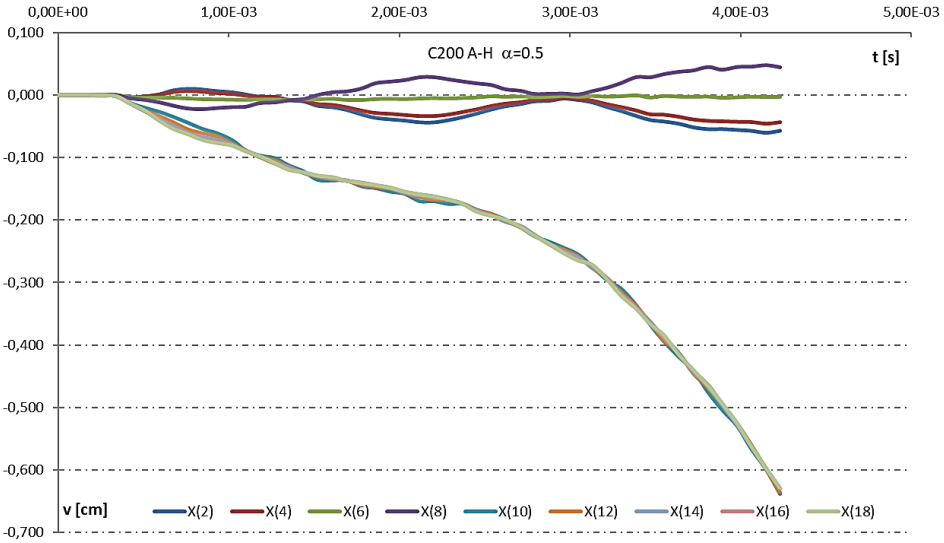

Fig. 6_{3a}. Change in vertical displacements over time of the points at the lower edge of the deep beam at the load level $\alpha = 0.5$ — a limited time interval was applied to the results in Fig. 6_3

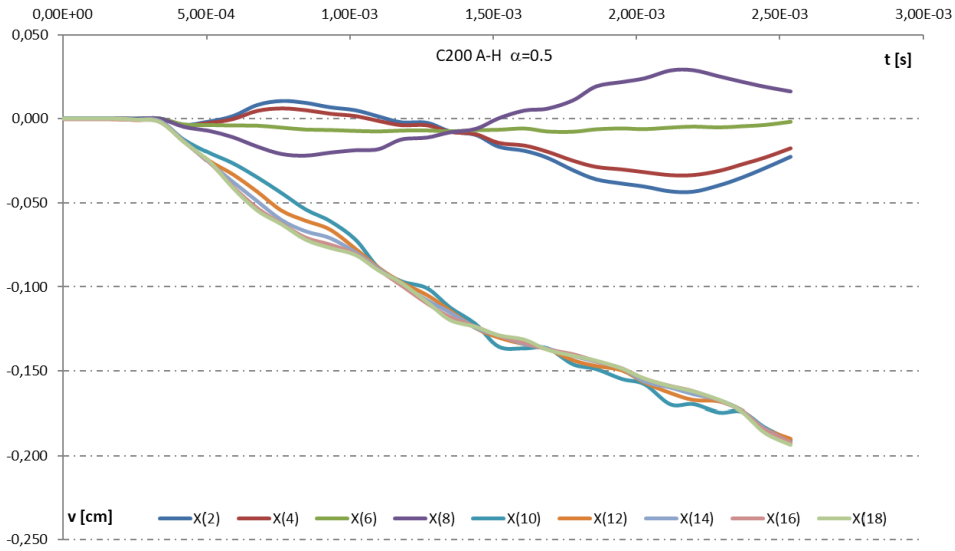

Fig. 6_{3b}. Change in vertical displacements over time of the points in the lower edge of the deep beam at the load level $\alpha = 0.5$ — a limited time interval was applied to the results in Fig. 6_{3a}

Fig. 7 shows the variability of the vertical displacement over time at the selected points at the upper edge of the deep beam at different load levels, $\alpha = P/P_0$. At load levels $a = 0.1$, $a = 0.2$, (Fig. 7_1), $a = 0.3$, (Fig. 7_2) and $a = 0.4$, (Fig. 7_3), similar to the deep beam reinforced with steel *A-III*, the maximum deflection was at point x_{306} of the span and the observed amplitude values of the vertical displacements decreased monotonously towards the support. In Fig. 7_4, which shows load level $a = 0.5$, further development of the concrete cracking area was found. There was an unlimited increase in the vertical displacements at the points in the vicinity of point x_{300}, indicative of the carrying capacity limit with a failure of the deep beam, similar to the deep beam reinforced with steel *A-III* at the load level $a = 0.6$.

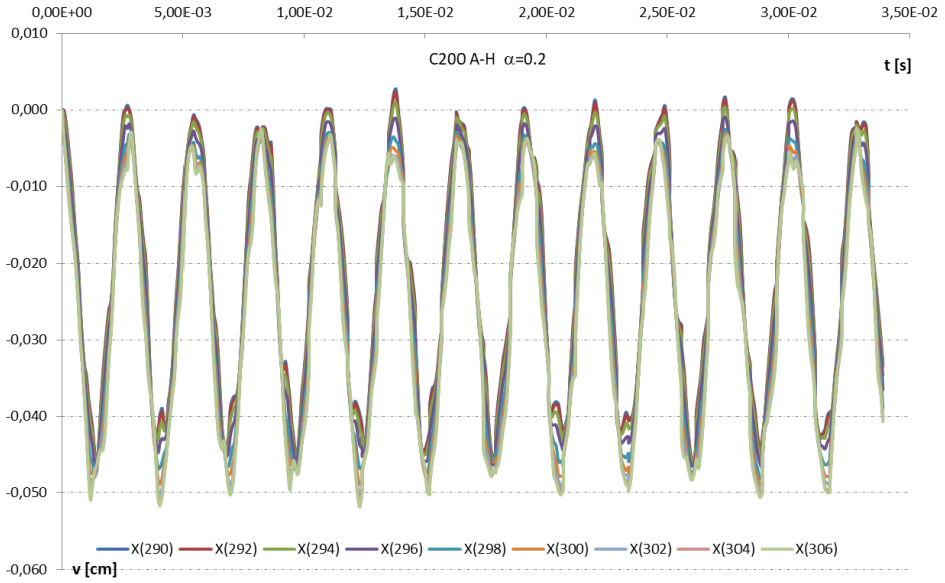

Fig. 7_1. Change in vertical displacements over time of the points at the upper edge of the deep beam at the load level $\alpha = 0.2$

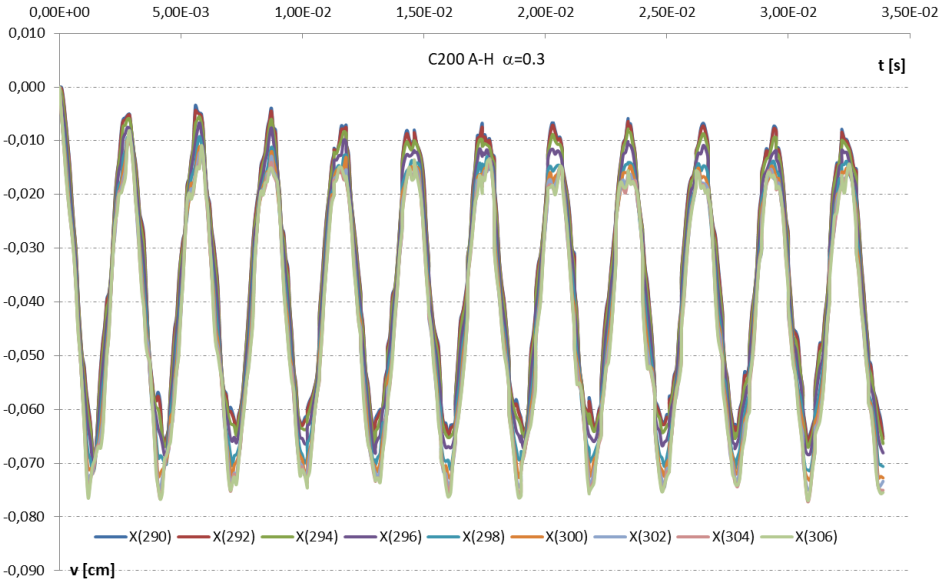

Fig. 7_2. Change in vertical displacements over time of the points at the upper edge of the deep beam at the load level $\alpha = 0.3$

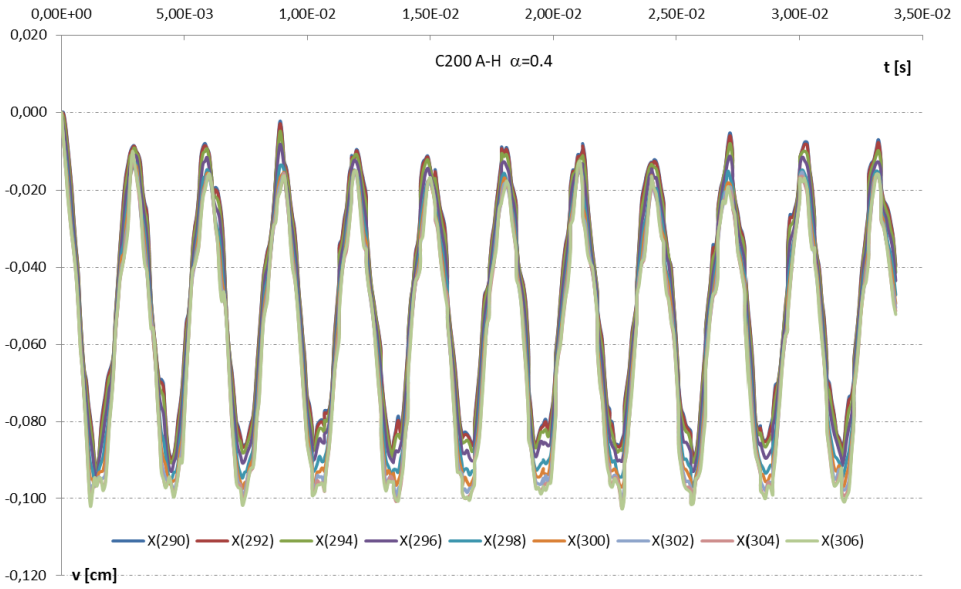

Fig. 7_3. Change in vertical displacements over time of the points at the upper edge of the deep beam at the load level $\alpha = 0.4$

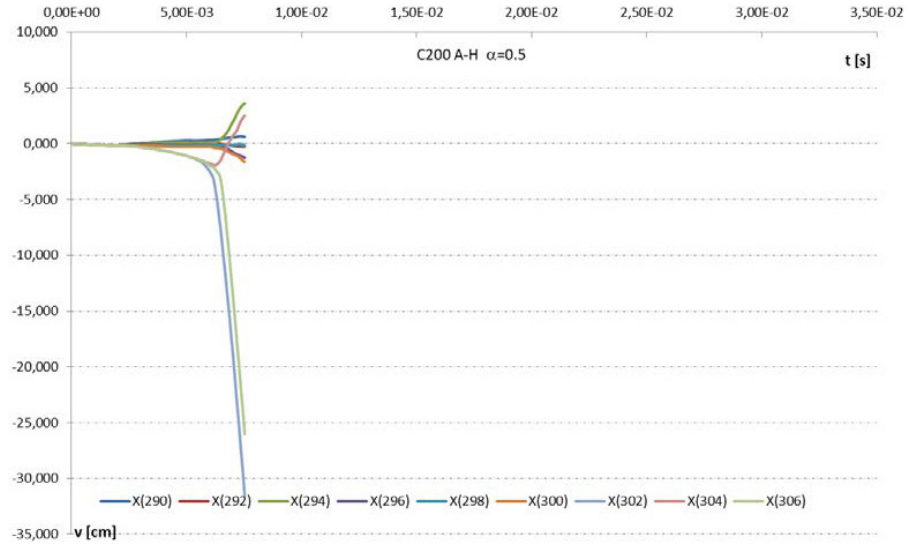

Fig. 7_4. Change in vertical displacements over time of the points at the upper edge of the deep beam at the load level $\alpha = 0.5$

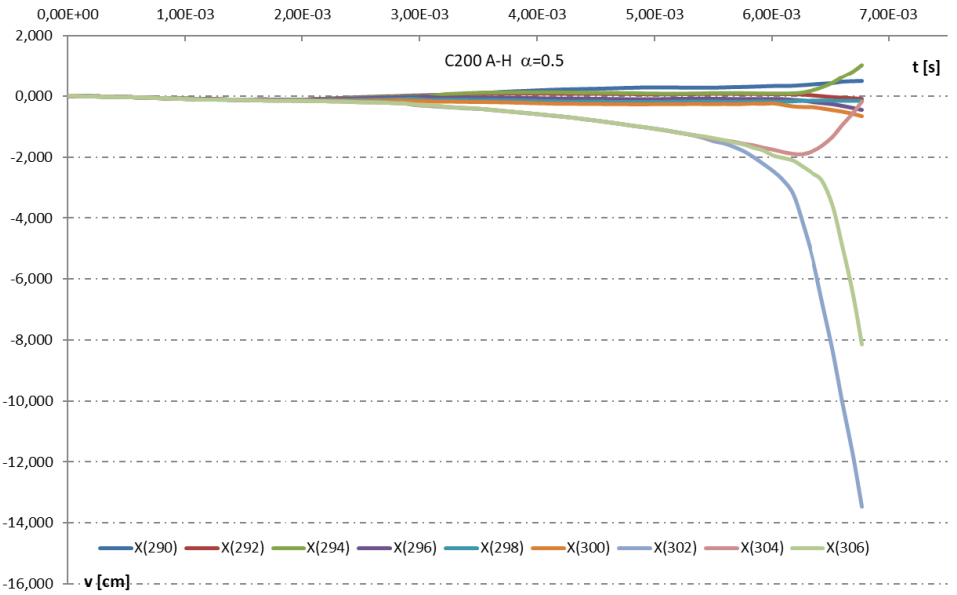

Fig. 7_{4a}. Change in vertical displacements over time of the points at the upper edge of the deep beam at the load level $\alpha = 0.5$ — a limited time interval was applied to the results in Fig. 7_4

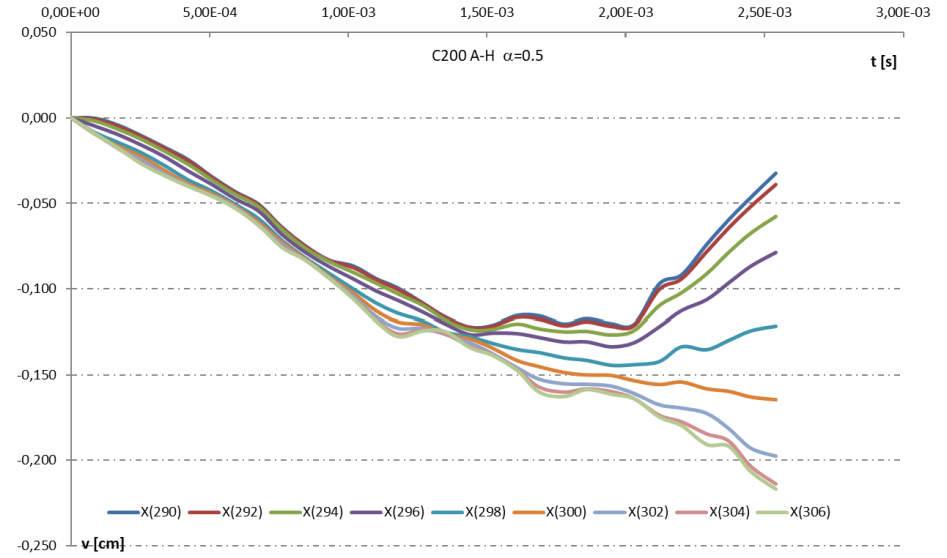

Fig. 7_{4b}. Change in vertical displacements over time of the points at the upper edge of the deep beam at the load level $\alpha = 0.5$ — a limited time interval was applied to the results in Fig. 7_{4a}

3. Conclusion — summary of Part Two

The work demonstrated the analysis of the displacement state of rectangular concrete deep beams made of very high strength concrete and steel of increased strength, under dynamic loads, including the physical non-linearity of the construction materials: concrete and reinforcing steel. A displacement dynamic state analysis of the reinforced concrete deep beam was carried out as a function of the two selected parameters, which defined the effects of the reinforced concrete structural element: concrete strength and steel strength. A very high-strength concrete, class *C200,* was selected, with two reinforcing steel classes: standard and increased strength. The deformation analysis of the deep beam was carried out by observing the changes in vertical displacement at selected points on the lower and upper edges of the deep beam and in the central section. The analysis established that increasing the strength of the reinforced steel can affect the mechanism of effort and failure of a concrete deep beam by a varied process involving the concentration and change in crack areas of the concrete matrix. The *C100* concrete deep beam reinforced with standard class steel (see [10]) led to the development of crack areas in two zones, the shear zone and the span zone. Replacement of the *C100* concrete with *C200* concrete changed the mechanism of effort in the deep beam. After the replacement, the propagation of crack areas only occurred in the shear zone of the deep beam. The change of concrete class did not change the relative level of the dynamic carrying capacity of the deep beams: it was at the load level $a = 0.5$ for the *C100* and *C200* concrete deep beams. However, the *C200* concrete deep beam featured a differentiated dynamic carrying capacity, a result of the reinforcing steel. For the standard reinforcing steel, class A-III, the maximum load level was found at $a = 0.5$. For the increased-strength reinforcing steel, class A-H, the maximum load level was found at $a = 0.4$. The results confirmed the necessity of investigating the effect of the constitutive model parameters of very high-strength concrete and increased-strength steel on the load mechanism of reinforced concrete elements. A full analysis of the effect of the changes in the strength parameters of steel on the deformation of the deep beams evaluated in this research requires additional analyses with changed parameters of the high-strength concrete. This analysis will be the subject of the next paper, on deep beams made of *C200* and *C300* concrete grades.

The work was created as a result of the research tasks carried out under Statutory Research no. 934 at the Faculty of Civil Engineering and Geodesy of the Military University of Technology.

Received December 5, 2017. Revised February 8, 2018.

Paper translated into English and verified by company SKRIVANEK sp. z o.o., 22 Solec Street, 00-410 Warsaw, Poland.

REFERENCES

[1] Cichorski W., Stolarski A., *Metoda analizy niesprężystego zachowania tarczy żelbetowej obciążonej dynamicznie*, Biuletyn WAT, 49, 10, 2000, 5-30.

[2] Stolarski A., *Model dynamicznego odkształcania betonu*, Archiwum Inżynierii Lądowej, 37, 3-4, 1991, 405-447.

[3] Cichorski W., Stolarski A., *Modelling of inelastic behaviour of reinforced concrete deep beam*, Journal of Achievements in Materials and Manufacturing Engineering, 44 (1), 2016, 37-44.

[4] Stolarski A., Cichorski W., *Influence of high strength of concrete and reinforced steel on dynamic behaviour of reinforced concrete deep beams*, Proceedings of the 12rd International Conference on Shock & Impact Loads on Structures, Singapore, 15 — 16 June 2017, 159- 168.

[5] Kleiber M., *Metoda elementów skończonych w nieliniowej mechanice kontinuum*, PWN, Warszawa, 1985.

[6] Leonhardt F., Walther R., *Wandartige träger*, Report, Deutscher Asschüb für Stahlbeton, 229, Berlin, Germany, 1966.

[7] Cichorski W., Stolarski A., *Analizy stanu przemieszczenia niesprężystej tarczy żelbetowej obciążonej statycznie*, Biuletyn WAT, 50, 5, 2001, 5-20.

[8] Stolarski A., Cichorski W., *Oszacowanie nośności tarczy żelbetowej z uwzględnieniem betonu bardzo wysokiej wytrzymałości*, Biuletyn WAT, 51, 2, 2002, 49-67.

[9] Cichorski W., Stolarski A., *Analizy wytężenia tarczy żelbetowej z materiałów konstrukcyjnych bardzo wysokich wytrzymałości*, Biuletyn WAT, 65, 4, 2016, 143-165.

[10] Cichorski W., *Analysis of dynamic displacement of reinforced concrete deep beams made of high strength concrete*, Part 1: *Analysis of dynamic displacement of a reinforced concrete deep beam made of high strength C100 grade concrete*, Biuletyn WAT, 67, 1, 2018, 141-174.

[11] Winnicki A., Pearce C.J. and Bićanić N., *Viscoplastic Hoffman consistency model for concrete*, Comput. & Struct., 2001, 79, 7-19.

[12] Marzec I., Tejchman J., Winnicki A., *Computational simulations of concrete behaviour under dynamic conditions using elasto-visco-plastic model with non-local softening*, Computers & Concrete, 2015, 15 (4), 515-545.

W. CICHORSKI

Analiza dynamicznego przemieszczenia tarcz żelbetowych z betonu wysokiej wytrzymałości

Część II: Analiza dynamicznego przemieszczenia tarczy żelbetowej z betonu wysokiej wytrzymałości klasy *C200*

Streszczenie. W pracy przedstawiono analizę stanu przemieszczenia prostokątnych tarcz żelbetowych wykonanych z betonu bardzo wysokiej wytrzymałości klasy *C200* obciążonych dynamicznie z uwzględnieniem fizycznych nieliniowości materiałów konstrukcyjnych: betonu i stali zbrojeniowej. Analiza została przeprowadzona na podstawie metody zaprezentowanej w pracy [1]. Przedstawiono wyniki rozwiązań numerycznych ze szczególnym uwzględnieniem stanu przemieszczenia tarczy. Przeprowadzono analizę porównawczą wpływu betonu wysokiej wytrzymałości i stali podwyższonej wytrzymałości na tarczy poprzez porównanie uzyskanych wyników dla tarczy z betonu klasy *C200* z wynikami uzyskanymi dla tarczy żelbetowej wykonanej z betonu klasy *C100* zamieszczonymi w pracy [10].

Słowa kluczowe: mechanika konstrukcji, konstrukcje żelbetowe, tarcze, obciążenie dynamiczne, nieliniowość fizyczna

DOI: 10.5604/01.3001.0012.0952